The Astronomical Journal, 146:54 (15pp), 2013 September doi:10.1088/0004-6256/146/3/54

ENIGMATIC RECURRENT PULSATIONAL VARIABILITY OF THE ACCRETING WHITE DWARF EQ LYN (SDSS J074531.92+453829.6)

Anjum S. Mukadam[1,2], D. M. Townsley[3], Paula Szkody[1,2], B. T. Gänsicke[4], J. Southworth[5], T. Brockett[3], S. Parsons[4], J. J. Hermes[6,7], M. H. Montgomery[6,7,8], D. E. Winget[6,7], S. Harrold[6,7], G. Tovmassian[9], S. Zharikov[9], A. J. Drake[10], A. Henden[11], P. Rodriguez-Gil[12,13], E. M. Sion[14], S. Zola[15,16], T. Szymanski[15], E. Pavlenko[17], A. Aungwerojwit[18,19], and S.-B. Qian[20]
[1] Department of Astronomy, University of Washington, Seattle, WA 98195-1580, USA
[2] Apache Point Observatory, 2001 Apache Point Road, Sunspot, NM 88349-0059, USA
[3] Department of Physics and Astronomy, The University of Alabama, Tuscaloosa, AL 35487, USA
[4] Department of Physics, University of Warwick, Coventry CV4 7AL, UK
[5] Astrophysics Group, Keele University, Staffordshire ST5 5BG, UK
[6] Department of Astronomy, University of Texas at Austin, Austin, TX 78759, USA
[7] McDonald Observatory, Fort Davis, TX 79734, USA
[8] Delaware Asteroseismic Research Center, Mt. Cuba Observatory, Greenville, DE 19807, USA
[9] Observatorio Astrónomico Nacional SPM, Instituto de Astronomía, Universidad Nacional Autónoma de México, Ensenada, BC, Mexico
[10] Department of Astronomy and the Center for Advanced Computing Research, California Institute of Technology, Pasadena, CA 91225, USA
[11] American Association of Variable Star Observers, 25 Birch Street, Cambridge, MA 02138, USA
[12] Departamento de Astrofísica, Universidad de La Laguna, La Laguna, E-38204 Santa Cruz de Tenerife, Spain
[13] Isaac Newton Group of Telescopes, Apartado de Correos 321, E-38700 Santa Cruz de La Palma, Spain
[14] Department of Astronomy and Astrophysics, Villanova University, Villanova, PA 19085, USA
[15] Astronomical Observatory, Jagiellonian University, ul. Orla 171, PL-30-244 Krakow, Poland
[16] Mount Suhora Observatory, Pedagogical University, ul. Podchorazych 2, PL-30-084 Krakow, Poland
[17] Crimean Astrophysical Observatory, Crimea 98409, Ukraine
[18] Department of Physics, Faculty of Science, Naresuan University, Phitsanulok 65000, Thailand
[19] ThEP Center, CHE, 328 Si Ayutthaya Road, Bangkok 10400, Thailand
[20] National Astronomical Observatories/Yunnan Observatory, Chinese Academy of Sciences, P.O. Box 110, 650011 Kunming, China
Received 2013 March 9; accepted 2013 June 17; published 2013 August 2

ABSTRACT

Photometric observations of the cataclysmic variable EQ Lyn (SDSS J074531.92+453829.6), acquired from 2005 October to 2006 January, revealed high-amplitude variability in the range 1166–1290 s. This accreting white dwarf underwent an outburst in 2006 October, during which its brightness increased by at least five magnitudes, and it started exhibiting superhumps in its light curve. Upon cooling to quiescence, the superhumps disappeared and it displayed the same periods in 2010 February as prior to the outburst within the uncertainties of a couple of seconds. This behavior suggests that the observed variability is likely due to nonradial pulsations in the white dwarf star, whose core structure has not been significantly affected by the outburst. The enigmatic observations begin with an absence of pulsational variability during a multi-site campaign conducted in 2011 January–February without any evidence of a new outburst; the light curve is instead dominated by superhumps with periods in the range of 83–87 minutes. Ultraviolet *Hubble Space Telescope* time-series spectroscopy acquired in 2011 March reveals an effective temperature of 15,400 K, placing EQ Lyn within the broad instability strip of 10,500–16,000 K for accreting pulsators. The ultraviolet light curve with 90% flux from the white dwarf shows no evidence of any pulsations. Optical photometry acquired during 2011 and Spring 2012 continues to reflect the presence of superhumps and an absence of pulsations. Subsequent observations acquired in 2012 December and 2013 January finally indicate the disappearance of superhumps and the return of pulsational variability with similar periods as previous data. However, our most recent data from 2013 March to May reveal superhumps yet again with no sign of pulsations. We speculate that this enigmatic post-outburst behavior of the frequent disappearance of pulsational variability in EQ Lyn is caused either by heating the white dwarf beyond the instability strip due to an elevated accretion rate, disrupting pulsations associated with the He II instability strip by lowering the He abundance of the convection zone, free geometric precession of the entire system, or appearing and disappearing disk pulsations.

Key words: novae, cataclysmic variables – stars: dwarf novae – stars: individual (EQ Lyn, SDSSJ074531.92+453829.6) – stars: oscillations – stars: variables: general – white dwarfs

Online-only material: color figures, supplemental data

1. INTRODUCTION

Cataclysmic variables are formed from two main-sequence stars evolving through a common envelope phase that decreases their separation and reduces the orbital period to hours via a loss of angular momentum. The donor star is a late-type secondary, filling its Roche lobe and transferring mass via the inner Lagrangian point to the accreting star, a white dwarf (primary). Angular momentum is lost initially via magnetic braking, and subsequently through the emission of gravitational radiation at orbital periods less than two hours (Warner 1995). White dwarfs with hydrogen-dominant donor stars evolve to an orbital period minimum near 80 minutes (Gänsicke et al. 2009; Uemura et al. 2010), while white dwarfs with helium-dominant donor stars achieve even shorter periods ranging from an hour to extreme cases at 5 minutes (e.g., Nelemans 2005; Roelofs et al. 2010; Breedt et al. 2012).

Due to the low rate of mass transfer $\sim 10^{-11}\ M_{\odot}\ \mathrm{yr}^{-1}$ near the orbital period minimum (Howell et al. 1995; Kolb & Baraffe 1999), the white dwarf is the source of most of the optical

light observed from a cataclysmic variable (Gänsicke et al. 1999; Szkody et al. 2007). Photometric variations consistent with nonradial g-mode pulsations were first discovered in the accreting white dwarf GW Lib in 1998 (Warner & van Zyl 1998; van Zyl et al. 2004). Follow-up photometry of other cataclysmic variables near the orbital period minimum have shown that several systems exhibit variability in the same regime as white dwarf pulsations (e.g., Vanlandingham et al. 2005; Araujo-Betancor et al. 2005; Gänsicke et al. 2006; Mukadam et al. 2007a; Pavlenko 2009; Patterson et al. 2008; Szkody et al. 2010). The potential of nonradial pulsations in accreting white dwarfs has opened a new venue of opportunity to learn about the stellar parameters of these stars using asteroseismic techniques (Townsley et al. 2004). A unique model fit to the observed periods of the variable white dwarf can allow a measurement of the stellar mass, core composition, age, rotation rate, magnetic field strength, and distance (Winget & Kepler 2008; Fontaine & Brassard 2008). Constraining the population, mass distribution, and evolution of accreting white dwarfs is also important in the context of understanding SN Type Ia progenitors.

2. BACKGROUND

Non-interacting hydrogen atmosphere (DA) white dwarfs are observed to pulsate in a narrow instability strip located within the temperature range 10,800–12,300 K for $\log g \approx 8$ (Koester & Holberg 2001; Bergeron et al. 2004; Mukadam et al. 2004; Gianninas et al. 2006), and are known as the ZZ Ceti stars. Arras et al. (2006) investigate the temperature range in which models of accreting white dwarfs with a wide range of masses and helium enrichment from the donor star would be pulsationally unstable. They find a H/He I instability strip for accreting model white dwarfs with a blue edge near $\leqslant$12,000 K for a 0.6 $M_{\odot}$ star. Although this H/He I strip for accreting white dwarfs is expected to be similar to the well-established ZZ Ceti instability strip in some respects, there are also several fundamental differences. The helium and metal-enriched envelopes of the models of accreting pulsators have H/He I ionization zones, while ZZ Ceti stars pulsate due to H ionization within their pure H envelopes. For accreting model white dwarfs with a high He abundance ($>$0.38), Arras et al. (2006) find a second hotter instability strip at $\approx$15,000 K due to He II ionization. These strips are expected to merge for an He abundance higher than 0.48, creating a broad instability strip. Szkody et al. (2007, 2010, 2012) are pioneering the effort to empirically establish the pulsational instability strip for accreting pulsators and their preliminary results indicate a broad instability strip in the temperature range of 10,500–16,000 K.

Shortly after Szkody et al. (2006) discovered that EQ Lyn (SDSS J074531.92+453829.6) is a cataclysmic variable, Mukadam et al. (2007a) found high-amplitude variations in their follow-up photometry of this faint ($g = 19.05$) accreting white dwarf. We will henceforth use the term "pulsational variability" to describe such observations of EQ Lyn, implying observed variability consistent with nonradial white dwarf pulsations. This is presently the most feasible model, even though it has its own set of unanswered questions.

The light curves acquired on 16 nights over a duration of 3.5 months between 2005 October and 2006 January reveal high-amplitude non-sinusoidal mono-periodic variations. Although only a single period was observed on any given night, different nights reveal the excitation of different periods within the range of 1166–1290 s. This phenomenon can be related to amplitude modulation because new frequencies get excited while previously observed frequencies die down indicating the changing amplitude of each mode.

3. ORBITAL PERIOD DETERMINATION

We obtained 17 spectra of EQ Lyn on the 2009 February 17, using the ISIS grating spectrograph installed at the William Herschel Telescope at La Palma, Spain, for a duration of 179 minutes before poor weather curtailed the observations. Each 600 s exposure consists of two spectra obtained simultaneously using the two arms of the instrument. The CCDs were binned by factors of two (spectral) and three (spatial) to limit the impact of readout noise on the observations. The blue arm, equipped with the R600B grating, has a wavelength coverage of 4190–4990 Å at a reciprocal dispersion of 0.45 Å per binned pixel and a resolution of approximately 1 Å. The red arm with the R316R grating covers 5760–8890 Å with a reciprocal dispersion of 1.85 Å per binned pixel and a resolution of approximately 3.5 Å.

The data were reduced and the spectra optimally extracted using the PAMELA[21] code (Marsh 1989) and the Starlink[22] packages FIGARO and KAPPA. Copper–neon and copper–argon arc lamp exposures were taken every hour during our observations and the wavelength calibration for each science exposure was linearly interpolated from the two arc observations bracketing it. We removed the telluric lines and calibrated the flux of the target spectra using observations of BD +75,325.

As in the previously acquired Sloan Digital Sky Survey (SDSS) spectrum (Szkody et al. 2006), the average spectrum of EQ Lyn (Figure 1) shows strong double-peaked Balmer-line emission, within wide absorption profiles arising from the photosphere of the white dwarf. Several weak He I emission lines are visible, and the He II 4686 Å line is also marginally detectable. The Paschen and Ca II infrared triplet lines also show emission. Figure 1 reveals the O I triplet near 7774 Å (Friend et al. 1988) as well as the Paschen 12 emission near 8750 Å, but no spectral features from the secondary star are visible.

We measured radial velocities from the Hα emission using the double-Gaussian method of Schneider & Young (1980), finding consistent results for a wide range of Gaussian widths and separations. The resulting orbital period is 79.5 $\pm$ 0.3 minutes, where the error bar encompasses all the values found for reasonable combinations of Gaussian widths and separations. We also studied the Hβ emission, obtaining more scattered radial velocities and an orbital period consistent with that from the Hα emission, although slightly shorter in absolute terms. A plot of the Hα radial velocities is shown in Figure 2.

We used this orbital period measurement to combine our spectra into 10 phase bins. The Hα emission line profile is shown in trailed and stacked form in Figure 3. The double-peaked emission can be seen to vary in velocity, and the S-wave due to the bright spot on the accretion disk is just about visible as changes in the relative strengths of the blue and red peaks through the orbit. We also show the Hβ and Hγ line profiles in trailed form in Figure 4.

4. CESSATION OF PULSATIONS AFTER AN OUTBURST

The cataclysmic variable EQ Lyn underwent an outburst in 2006 October, causing its brightness to increase by more than

[21] PAMELA and MOLLY were written by T.R.M. and can be obtained from http://www.warwick.ac.uk/go/trmarsh.
[22] The Starlink software and documentation can be obtained from http://starlink.jach.hawaii.edu/.

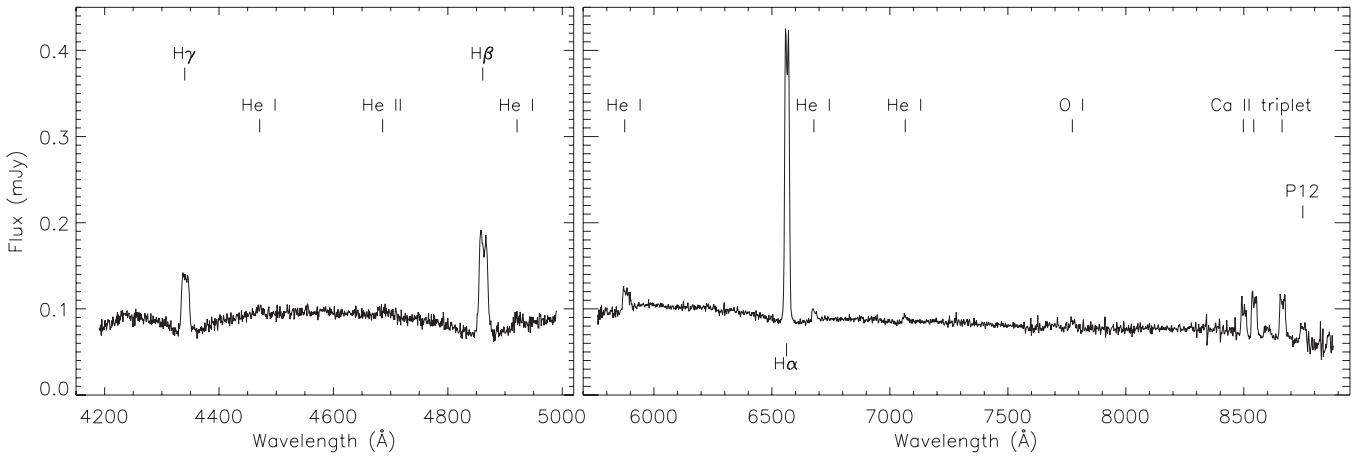

Figure 1. Flux-calibrated average spectrum of EQ Lyn is shown with the most significant emission and absorption features labeled. Data from the blue arm of ISIS are shown in the left panel, and from the red arm in the right panel.

(Supplemental data for this figure are available in the online journal.)

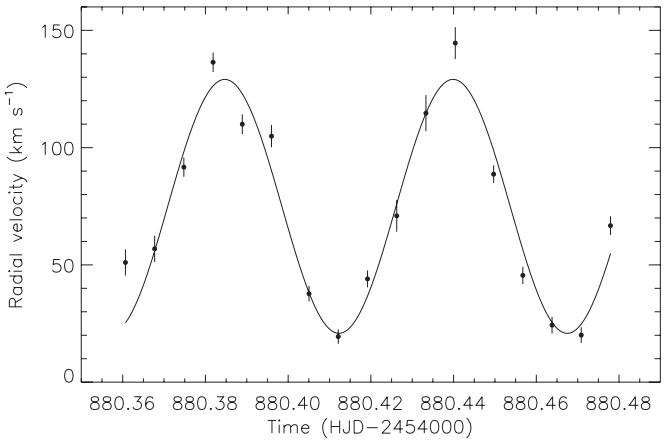

Figure 2. Hα emission line radial velocities (filled circles) compared to the best-fit spectroscopic orbit (solid line).

(Supplemental data for this figure are available in the online journal.)

five orders of magnitude, as shown by photometry acquired during the Catalina Real-Time Transient Survey (CRTS; Drake et al. 2009) in Figure 5. The heated white dwarf showed superhumps in subsequent optical data, without any signs of pulsational variability even in ultraviolet observations acquired in 2007 November (Szkody et al. 2010; Mukadam et al. 2011b). The co-added spectrum acquired using the *Hubble Space Telescope* (*HST*) indicated an effective temperature of 17,000 ± 1000 K (Szkody et al. 2010), implying that the white dwarf was still too hot to pulsate even a year after outburst. It was not until 2010 February that pulsational variability was again observed in the system at precisely the same set of periods as prior to the outburst (Mukadam et al. 2011b).

We performed a least-squares analysis of all the previous pulsational data on EQ Lyn. The light curves typically reveal a high-amplitude long period, accompanied by multiple harmonics of diminishing amplitude; these harmonics show smaller uncertainties in period determination due to the larger number of cycles compared to the dominant fundamental period. During the reanalysis, we forced the frequencies of the respective harmonics to be a multiple of the fundamental frequency. This leads to a significant reduction in the uncertainty of measuring the fundamental period, as shown by the values in Table 1.

Table 1
Dominant Periods Displayed by EQ Lyn since Its Discovery, Force-fit with the Constraint that Observed Harmonics Have to be a Multiple of the Fundamental Frequency

Date (UTC)	Fundamental Period (s)
2005 Oct 14	1186 ± 13
2005 Nov 30	1233.3 ± 6.9
2005 Dec 30	1209.1 ± 1.5
2006 Jan 1	1202.3 ± 3.9
2006 Jan 2	1222 ± 12
2006 Jan 4	1234.0 ± 2.3
2006 Jan 5	1228.6 ± 1.7
2006 Jan 6	1199.50 ± 0.62
2006 Jan 7	1199.39 ± 0.94
2006 Jan 8	1192.8 ± 1.1
2006 Jan 9	1232.5 ± 1.5
2006 Jan 20	1216.1 ± 1.6
2006 Jan 21	1221.1 ± 2.1
2006 Jan 22	1290 ± 40
2006 Jan 23	1253.7 ± 3.4
2006 Jan 30	1220.5 ± 5.5
2010 Feb 13	1232.1 ± 4.4
2010 Mar 4	1201.0 ± 1.3
2010 Mar 5	1216.92 ± 0.87
2010 Mar 13	1189.98 ± 0.49

Figure 6 shows the values of the fundamental period observed at different times before and after outburst, with vertical lines indicating how well most of the post-outburst periods match the pre-outburst observations within the uncertainties of 2.3 s. It is this discovery that leads us to believe that the unchanged periods are governed by the inner stellar structure, and the outburst does not perturb the white dwarf interior.

Another reason to reanalyze the previous data is to attempt to constrain the stellar mass using the period spacing of the observed modes (e.g., Winget et al. 1994). The apparent period spacing evident in Figure 6 is of the order of 10 s, which is significantly smaller compared to the observed values of 20–30 s in ZZ Ceti stars. However, since accreting white dwarfs are typically expected to exhibit rapid rotation, we could easily be misidentifying rotational splittings as adjacent radial order modes. It is also possible that some of these modes may be $\ell = 2$

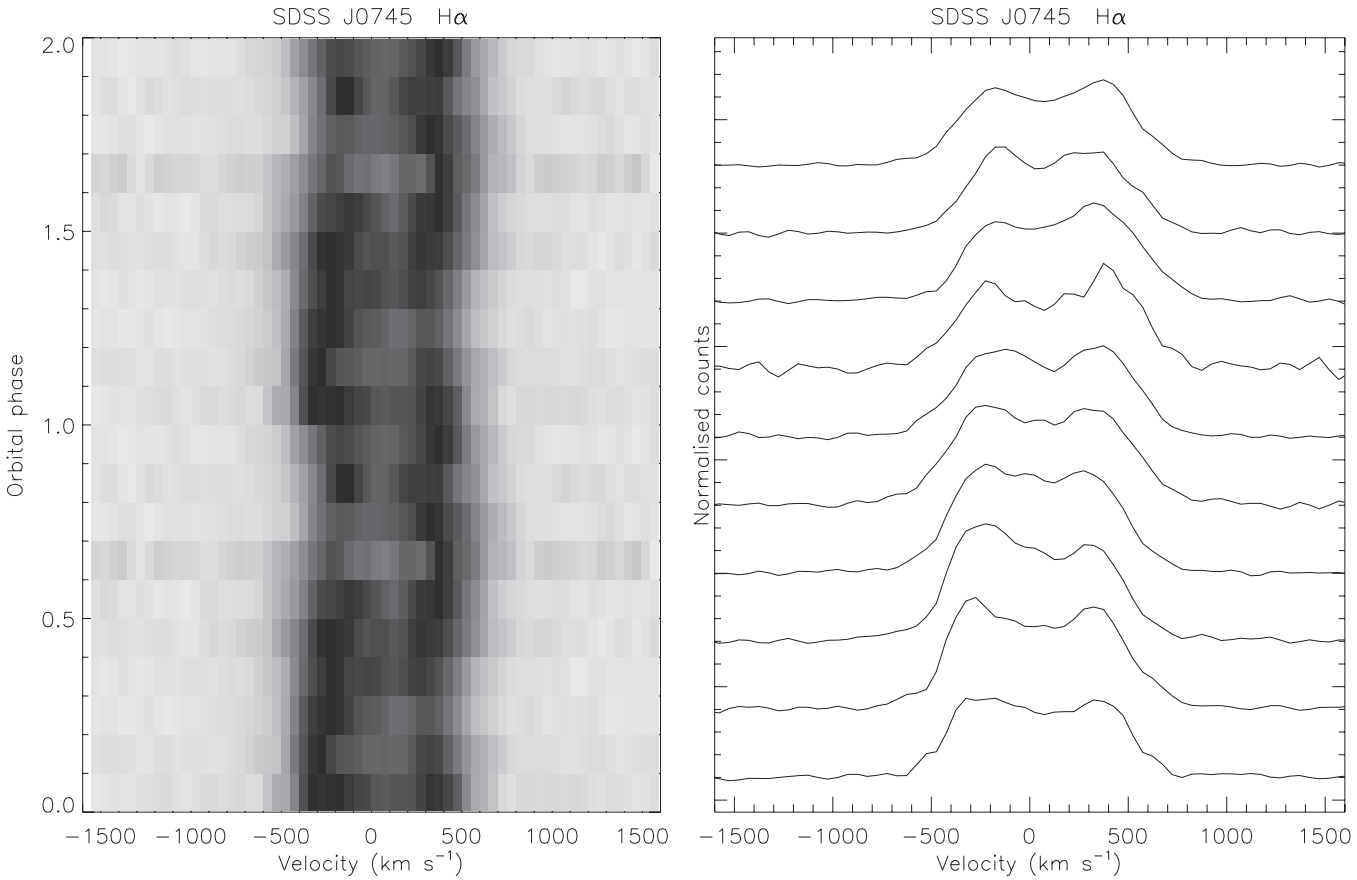

Figure 3. Phase-binned spectra of the Hα emission line for EQ Lyn are shown as a gray-scale trail (left) and stacked (right) in arbitrary flux units.

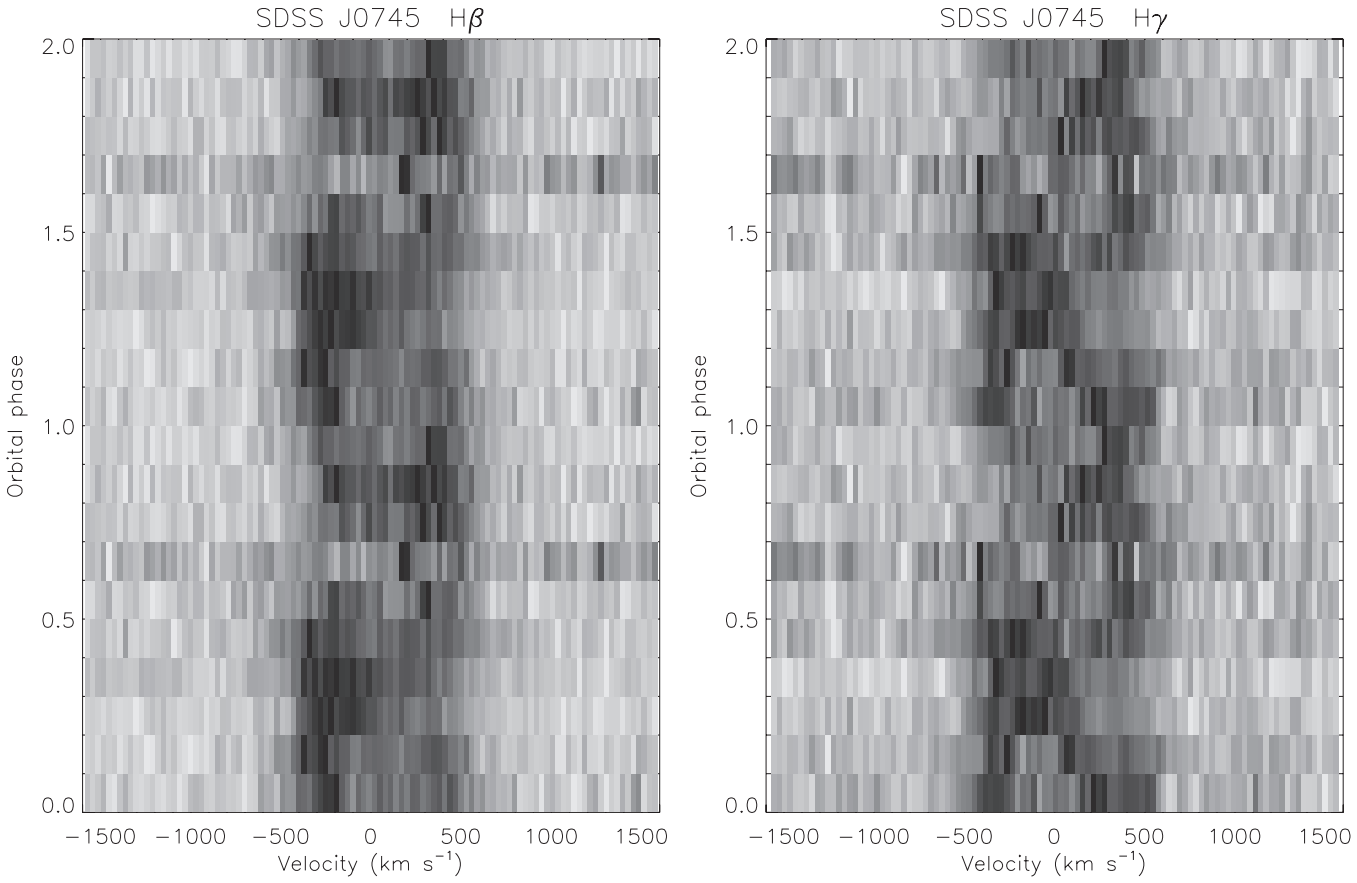

Figure 4. Phase-binned spectra of the Hβ and Hγ emission lines for EQ Lyn are shown as gray-scale trails.

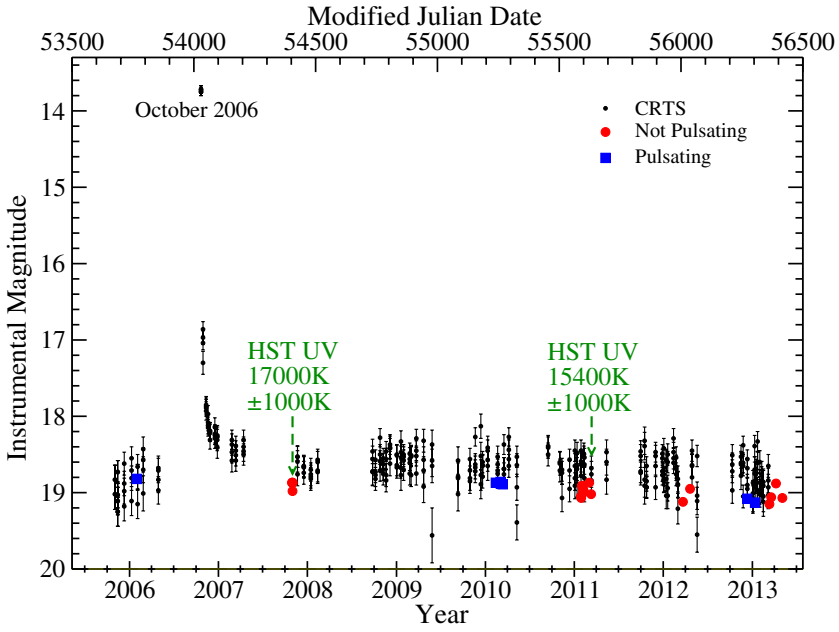

Figure 5. CRTS (Drake et al. 2009) light curve of EQ Lyn reveals the outburst of 2006 October as well as the absence of any subsequent outburst. Note that the magnitude determined during the *HST* observations from 2007 November is nearly the same as the value obtained during 2011 March observations in spite of the substantial difference of 1600 ± 1400 K in temperature.

(A color version and supplemental data for this figure are available in the online journal.)

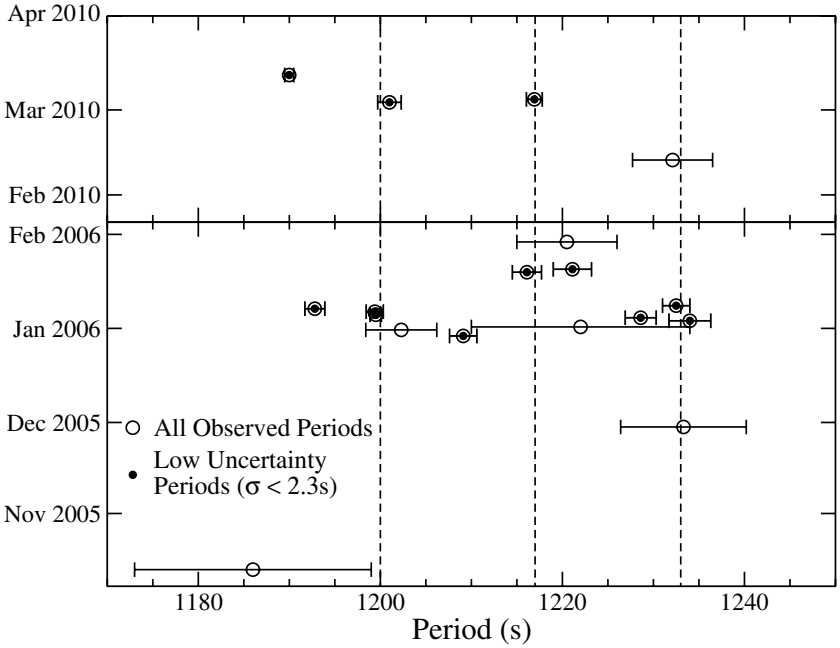

Figure 6. Most of the post-outburst pulsation periods match those observed prior to the outburst within the uncertainties of 2.3 s.

modes. Without a proper mode identification, we find ourselves unable to complete our goal of constraining the stellar mass using the period spacing.

Nonradial *g*-mode eigenfunctions of model white dwarfs with periods near 1200 s are likely to have high radial mode indices and should delve closer to the surface compared to low radial order modes. Assuming that the variability shown by EQ Lyn stems from nonradial *g*-modes, it is feasible that fluctuations in the daily accretion rate change the surface layers sufficiently to alter the observed frequencies by a few seconds. Should this effect be significant, it could very well account for why it is difficult to establish a clear period spacing from Figure 6.

5. CESSATION OF PULSATIONAL VARIABILITY WITHOUT AN OUTBURST DURING A MULTI-SITE OPTICAL CAMPAIGN

We organized a multi-site optical campaign on EQ Lyn in 2011 January–February with the purpose of obtaining high signal-to-noise (S/N) data to employ the light curve fitting technique (Montgomery 2005; Montgomery et al. 2010) in order to probe the stellar convection zone. Nonlinear pulse shapes, as observed in EQ Lyn, can be introduced physically by relatively thick convection zones (Brickhill 1992a; Brassard et al. 1995; Wu 2001; Montgomery 2005); fitting a light curve successfully

Table 2
Journal of Photometric Observations

Telescope Aperture	Instrument	Start Time (UTC)	End Time (UTC)	Exposure Time (s)	Time Resolution (s)	Number of Images	Filter
APO 3.5 m[a]	Agile	2011 Jan 28 01:30:40	01:56:25	15	15	104	BG40
APO 3.5 m	Agile	2011 Jan 28 02:01:30	04:03:30	15	15	489	BG40
APO 3.5 m	Agile	2011 Jan 28 04:08:12	12:36:13	17	17	1794	BG40
APO 3.5 m	Agile	2011 Jan 29 02:41:32	04:42:17	15	15	484	BG40
OAN-SPM 1.5 m[a]	Ruca	2011 Feb 1 03:22:29	11:26:46	60	67.7	430	BG40
SARA 0.9 m[a]	Apogee	2011 Feb 1 05:33:24	12:30:27	120	133.8	188	None
INT 2.5 m[a]		2011 Feb 2 21:07:09.6	04:27:32.6		44.7	593	
OAN-SPM 1.5 m	Ruca	2011 Feb 2 03:29:45	09:19:49	60	70.2	301	BG40
SARA 0.9 m	Apogee	2011 Feb 3 04:14:56	10:11:58	120	150.9	156	None
OAN-SPM 1.5 m	Ruca	2011 Feb 4 06:11:20	06:18:40	90	110.0	5	BG40
OAN-SPM 1.5 m	Ruca	2011 Feb 4 06:18:52	10:34:10	120	140.5	110	BG40
McD 2.1 m[a]	Argos	2011 Feb 5 02:18:18	10:18:18	30	30	961	BG40
OAN-SPM 1.5 m	Ruca	2011 Feb 5 03:43:00	09:02:13	90	110.1	175	BG40
SARA 0.9 m	Apogee	2011 Feb 6 02:07:51	11:39:47	120	143.6	245	None
OAN-SPM 1.5 m	Ruca	2011 Feb 6 04:01:28	08:57:03	90	110.2	162	BG40
OAN-SPM 1.5 m	Ruca	2011 Feb 7 03:06:00	10:57:24	90	132.9	185	BG40
McD 2.1 m	Argos	2011 Feb 8 01:45:36	08:31:36	30	30	813	BG40
APO 3.5 m	Agile	2011 Mar 11 02:35:54	03:36:54	60	60	62	BG40
APO 3.5 m	Agile	2011 Mar 11 03:38:52	07:05:22	30	30	414	BG40
FTN 2.0 m[a]	Spectral	2011 Mar 11 07:07:01.055	10:58:05.220	60		165	g
HST 2.0 m[a]	COS[a]	2011 Mar 13 06:31:11	07:10:52.184	2381.184	3	793	[b]
HST 2.0 m	COS	2011 Mar 13 08:06:57	08:58:42.184	3105.184	3	1035	[b]
APO 3.5 m	Agile	2011 Mar 15 02:11:31	02:42:01	30	30	62	BG40
APO 3.5 m	Agile	2011 Mar 15 02:48:57	02:56:27	30	30	16	BG40
APO 3.5 m	Agile	2011 Mar 15 03:01:24	04:29:24	60	60	89	BG40
APO 3.5 m	Agile	2011 Mar 15 04:31:24	07:01:24	30	30	301	BG40
APO 3.5 m	Agile	2012 Mar 22 07:17:28	10:10:16	12	12	865	BG40
McD 2.1 m	Raptor	2012 Apr 20 02:18:12	05:28:27	15	15	762	BG40
APO 3.5 m	Agile	2012 Dec 11 07:11:06	13:15:36	15	15	1459	BG40
APO 3.5 m	DIS[a]	2013 Jan 12 02:33:47.929	03:40:03.026	20	25.8	156	None
APO 3.5 m	Agile	2013 Mar 12 07:31:28	08:27:08	10	10	335	BG40
APO 3.5 m	Agile	2013 Mar 12 08:41:10	09:48:30	10	10	405	BG40
McD 2.1 m	Raptor	2013 Mar 19 02:13:30	05:15:00	30	30	364	BG40
APO 3.5 m	DIS	2013 Apr 8 02:25:46.997	03:45:03.721	15	21.0	226	None
APO 3.5 m	DIS	2013 Apr 8 03:45:32.022	07:09:52.321	20	26.0	473	None
APO 3.5 m	DIS	2013 May 4 03:39:05.784	04:55:55.295	25	29.9	155	None

Notes.
[a] The abbreviations correspond to: Apache Point Observatory (APO), Observatorio Astrónomico Nacional in San Pedro Martir (OAN-SPM), Southeastern Association for Research in Astronomy (SARA), Isaac Newton Telescope (INT), McDonald Observatory (McD), Faulkes Telescope North (FTN), *Hubble Space Telescope* (*HST*), Cosmic Origins Spectrograph (COS), and Dual Imaging Spectrograph (DIS).
[b] The wavelength ranges over which the spectra were summed to produce the *HST* ultraviolet light curve are: 1120–1208.4 Å, 1223.2–1295.6 Å, and 1312.2–1820 Å.

yields the thermal response timescale of the convection zone and the inclination angle of the pulsation axis, as well as the mode identification. Identifying the mode indices of observed pulsation periods is the first step in obtaining a unique model fit and determining fundamental stellar parameters using the technique of asteroseismology.

The journal of observations of our multi-site campaign as well as subsequent observations is shown in Table 2. We used a standard IRAF[23] (Tody 1993) reduction to extract sky-subtracted light curves from the CCD frames using weighted circular aperture photometry (O'Donoghue et al. 2000). After a preliminary reduction, we converted the data to fractional intensity ($\Delta I/I$) and the mid-exposure times of the CCD images to Barycentric Dynamic Time (TDB).

Light curve fitting is routinely performed for the non-interacting DA and DB pulsators (Montgomery et al. 2010; Provencal et al. 2012), and would have been conducted for the very first time on an accreting white dwarf pulsator. Unfortunately, light curves of EQ Lyn obtained during the campaign did not exhibit any evidence of pulsations, but were instead dominated by superhumps (see Figure 7).

5.1. Superhump Periods

Superhumps are photometric periods longer than the orbital period, believed to be caused by a precessing accretion disk. The class of SU UMa dwarf novae show three distinct stages of superhump evolution: an initial stage A with a long superhump period, a middle stage B with an increasing superhump period,

[23] IRAF is distributed by the National Optical Astronomy Observatory, which is operated by the Association of Universities for Research in Astronomy, Inc., under cooperative agreement with the National Science Foundation.

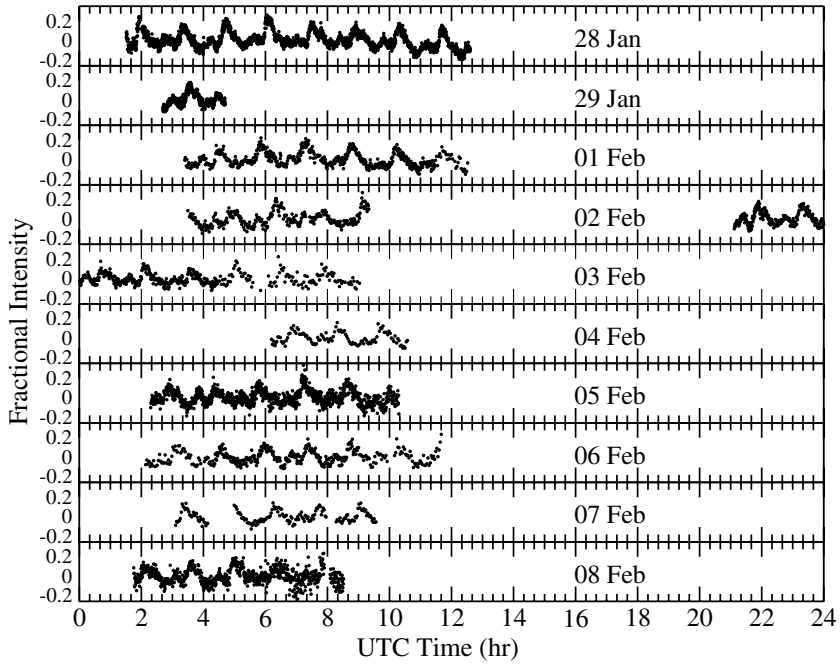

Figure 7. EQ Lyn light curves obtained during 2011 multi-site campaign reveal superhumps with no evidence of pulsations.
(Supplemental data for this figure are available in the online journal.)

and a late stage C with a slightly shorter and stable superhump period. WZ Sge type dwarf novae, a sub-class of SU UMa type dwarf novae, with low accretion rates are characterized by large-amplitude rare superoutbursts (Bailey 1979; Downes 1990; Howell et al. 1995; Kato et al. 2001). These outbursts increase the system brightness by ∼8 mag and typically occur on decade timescales. Well-observed WZ Sge type systems like GW Lib, V455 And, and SDSS J0804+5103 have shown superhumps well past their outbursts. These late superhumps observed after the superoutburst peaks are supposed to originate in the precessing eccentric disk near the tidal truncation (Kato et al. 2008). This implies that the eccentric disk continues to expand slowly after the end of stage B until it reaches the tidal truncation when the period gets stabilized (Kato et al. 2009).

The superhump periods we observed during the campaign lie in the range of 83–87 minutes (Table 3), longer than the orbital period of 79.5 minutes by about 8%. The last column of Table 3 indicates the superhump periods we obtain by forcing the frequencies of the respective harmonics to be a multiple of the fundamental frequency. This exercise utilizes the harmonics to improve the measurement of the fundamental period, reducing the spread in the observed nightly values. Figure 8 reveals the discrete Fourier transform (DFT) of the campaign light curve, which shows the superhump period of 85.77 minutes along with multiple harmonics. The superhump periods shown in Tables 3–5 over a duration of 16 months from 2011 January to 2012 April fall within the range of 83.6–86.8 minutes without any noticeable evolutionary increase. However, the short duration of our nightly observations do not allow for accurate measurements.

Gänsicke et al. (2009) analyzed 68 well-studied cataclysmic variables below the orbital period gap of 2.1–2.7 hr and updated the well-known linear relation between the orbital period and the superhump period observed in these systems during superoutbursts (e.g., Patterson et al. 2005). This linear correlation allows an indirect measurement of the orbital period from observed superhumps within an uncertainty of 2 minutes. Our measurements of the orbital and superhump periods make EQ Lyn an outlier in Figure 1 from Gänsicke et al. (2009), perhaps implying that the quiescent superhumps we observe in this system are of a different nature than ordinary superhumps shown by SU UMa dwarf novae during outbursts. These superhumps disappeared in 2010 February and March, when pulsational variability was observed in the light curves, and made their appearance again during the multi-site campaign when pulsations disappeared from the system.

6. MULTI-WAVELENGTH 2011 MARCH CAMPAIGN

The disappearance of pulsational variability during 2011 January–February campaign is puzzling, especially since the CRTS (Drake et al. 2009) did not detect any signs of a large outburst between 2010 March and 2011 January (Figure 5). Howell et al. (1995) show that large outbursts are rare near the orbital period minimum and occur at intervals of a decade or two for the low accretion rate of $\sim 10^{-11}\ M_{\odot}\ \mathrm{yr}^{-1}$. Due to gaps in the CRTS data, we could not rule out short normal outbursts that may have occurred when EQ Lyn was behind the Sun, although these are not typical at low accretion rates.

6.1. Ultraviolet Time-series Spectroscopy

With the primary purpose of obtaining an effective temperature of the white dwarf, we acquired two orbits of *HST*[24] ultraviolet time-series spectroscopy targeting EQ Lyn on 2011 March 13. Ultraviolet *HST* observations are necessary to obtain a reliable white dwarf temperature, as optical spectra contain a substantial contamination from the accretion disk. Szkody et al. (2010) calculate that accreting white dwarfs contribute 75%–89% of the ultraviolet flux, and about 42%–75% in the

[24] Based on observations made with the NASA/ESA *Hubble Space Telescope*, obtained at the Space Telescope Science Institute, which is operated by the Association of Universities for Research in Astronomy, Inc., under NASA contract NAS 5-26555. These observations are associated with the program HST-GO-11163.01-A.

Table 3
Optical Best-fit Periodicities Obtained in 2011 January–February

UT Date	Period (minutes)	Amplitude (mma)	Fundamental–Harmonic Period (minutes)
2011 Jan 28	83.160 ± 0.098	73.5 ± 1.3	83.588 ± 0.047
	41.935 ± 0.043	43.6 ± 1.3	
	27.873 ± 0.027	29.9 ± 1.3	
	20.927 ± 0.037	12.5 ± 1.3	
	16.220 ± 0.040	6.9 ± 1.3	
2011 Jan 29	76.4 ± 1.6	51.5 ± 3.1	
2011 Feb 1	87.15 ± 0.27	73.0 ± 2.2	86.80 ± 0.17
	43.23 ± 0.16	29.3 ± 2.2	
	28.885 ± 0.087	24.3 ± 2.2	
2011 Feb 2	86.85 ± 0.67	64.7 ± 3.5	85.73 ± 0.35
	42.20 ± 0.27	38.1 ± 3.5	
	28.75 ± 0.25	18.8 ± 3.5	
2011 Feb 2–3	86.07 ± 0.22	53.7 ± 1.8	85.847 ± 0.087
	42.622 ± 0.078	36.3 ± 1.8	
	28.665 ± 0.053	24.1 ± 1.8	
	21.522 ± 0.053	13.6 ± 1.8	
	17.250 ± 0.053	8.6 ± 1.8	
2011 Feb 4	84.38 ± 0.93	65.57 ± 3.8	84.72 ± 0.52
	42.37 ± 0.62	24.2 ± 3.8	
	28.37 ± 0.27	22.6 ± 3.8	
2011 Feb 5	87.15 ± 0.33	55.7 ± 2.0	85.80 ± 0.14
	68.88 ± 0.58	20.2 ± 2.0	
	42.40 ± 0.13	33.8 ± 2.0	
	28.557 ± 0.090	22.4 ± 2.0	
	21.50 ± 0.11	10.5 ± 2.0	
2011 Feb 6	84.85 ± 0.33	64.0 ± 2.6	84.65 ± 0.18
	42.29 ± 0.16	33.4 ± 2.6	
	28.16 ± 0.11	20.9 ± 2.6	
2011 Feb 7	84.02 ± 0.55	57.7 ± 3.3	84.87 ± 0.30
	57.6 ± 1.0	15.3 ± 3.4	
	42.33 ± 0.30	28.4 ± 3.2	
	28.52 ± 0.18	20.2 ± 3.1	
2011 Feb 8	84.55 ± 0.38	65.1 ± 2.7	84.88 ± 0.22
	42.42 ± 0.18	36.1 ± 2.7	
	36.25 ± 0.28	16.9 ± 2.7	
	28.63 ± 0.18	16.9 ± 2.7	
	20.55 ± 0.11	14.6 ± 2.6	
2011 Jan 28–Feb 8	85.7763 ± 0.0038	49.24 ± 0.89	85.7712 ± 0.0025
	79.9858 ± 0.0072	22.48 ± 0.89	
	42.8818 ± 0.0022	21.25 ± 0.89	
	41.3875 ± 0.0022	19.75 ± 0.89	
	27.91423 ± 0.00092	19.18 ± 0.82	
	21.3723 ± 0.0012	8.54 ± 0.82	
	14.20413 ± 0.00090	5.02 ± 0.82	

Table 4
Ultraviolet and Optical Best-fit Periodicities Obtained in 2011 March

Wavelength	UT Date	Period (minutes)	Amplitude (mma)	Fundamental–Harmonic Period (minutes)
Ultraviolet	2011 Mar 13	95.5 ± 2.3	45.2 ± 3.7	
Optical	2011 Mar 11	85.12 ± 0.52	64.3 ± 2.2	84.93 ± 0.38
		42.22 ± 0.32	26.7 ± 2.1	
		21.38 ± 0.11	20.4 ± 2.1	
Optical	2011 Mar 15	86.95 ± 0.52	74.8 ± 2.3	86.52 ± 0.33
		42.70 ± 0.28	36.1 ± 2.3	
		28.73 ± 0.18	24.6 ± 2.3	

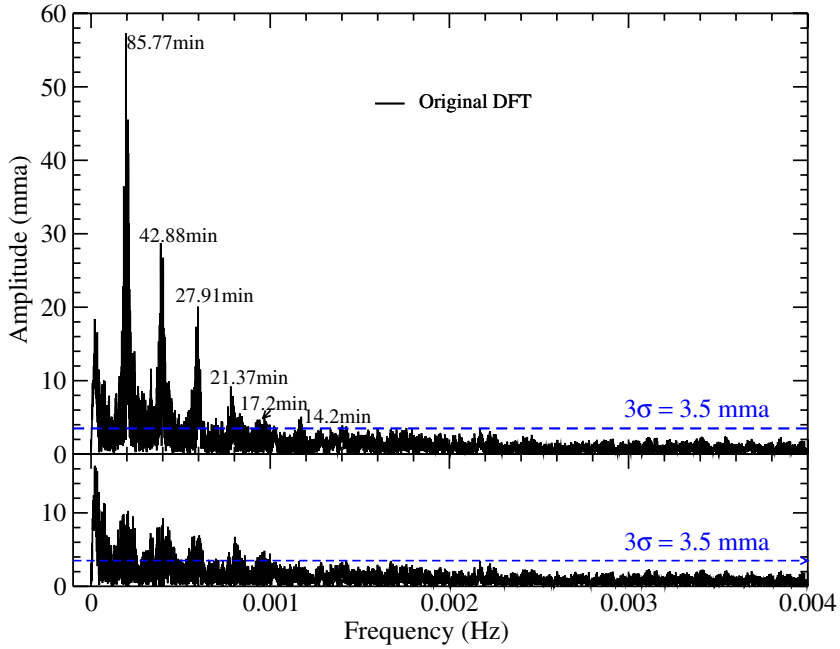

Figure 8. We show the original (top panel) and prewhitened (bottom panel) DFTs, obtained after subtracting out the superhump period of 85.77 minutes and its harmonics.

(A color version of this figure is available in the online journal.)

Table 5
Optical Best-fit Periodicities Obtained in 2012 and 2013

UT Date	Period	Amplitude (mma)	Fundamental–Harmonic Period
2012 Mar 22	87.17 ± 0.95 minutes	112.8 ± 2.8	
	51.20 ± 0.62 minutes	58.0 ± 2.9	
2012 Apr 20	84.72 ± 0.43 minutes	87.6 ± 1.9	84.40 ± 0.37 minutes
	41.98 ± 0.27 minutes	35.7 ± 1.9	
2012 Dec 11	1119.05 ± 0.66 s	64.5 ± 1.4	1117.78 ± 0.39 s
	558.13 ± 0.46 s	22.9 ± 1.4	
	372.49 ± 0.19 s	25.5 ± 1.4	
2013 Jan 12	1139 ± 22 s	35.8 ± 4.4	1127.4 ± 8.0 s
	573.5 ± 5.3 s	40.6 ± 4.3	
	368.9 ± 3.8 s	22.3 ± 4.3	
2013 Mar 12	59.0 ± 1.2 minutes	18.7 ± 1.6	
	26.82 ± 0.37 minutes	12.8 ± 1.6	26.50 ± 0.18 minutes
	13.053 ± 0.077 minutes	14.4 ± 1.6	
	1028.6 ± 6.2 s^{α}	18.4 ± 1.6	1070.8 ± 4.4 s
	547.0 ± 3.1 s^{α}	10.4 ± 1.6	
	358.8 ± 1.4 s^{α}	9.6 ± 1.6	
2013 Mar 19	83.4 ± 1.4 minutes	37.3 ± 2.5	82.28 ± 0.62 minutes
	40.20 ± 0.45 minutes	31.3 ± 2.4	
	29.82 ± 0.37 minutes	19.8 ± 2.4	
2013 Apr 8	88.28 ± 0.55 minutes	49.5 ± 1.8	87.13 ± 0.28 minutes
	42.95 ± 0.35 minutes	18.9 ± 1.8	
	28.75 ± 0.12 minutes	24.1 ± 1.8	
	21.77 ± 0.11 minutes	16.0 ± 1.8	
	36.63 ± 0.27 minutes^{β}	17.9 ± 1.8	
	17.228 ± 0.072 minutes^{β}	14.5 ± 1.8	
2013 May 4	89.4 ± 3.5 minutes	76.7 ± 4.2	

optical regime. We also obtained nearly simultaneous optical observations on March 11 and 15 for additional data over a relatively longer time base to help characterize the state of the system and improve the determination of any present periodicities.

The *HST* ultraviolet time-series spectra were obtained on 2011 March 13, using the Cosmic Origins Spectrograph (COS) equipped with the G140L grating at a plate scale of 0.″021 pixel^{-1} and a spectral resolution of 2500. The time-tag data were reduced using pyRAF routines of the STSDAS

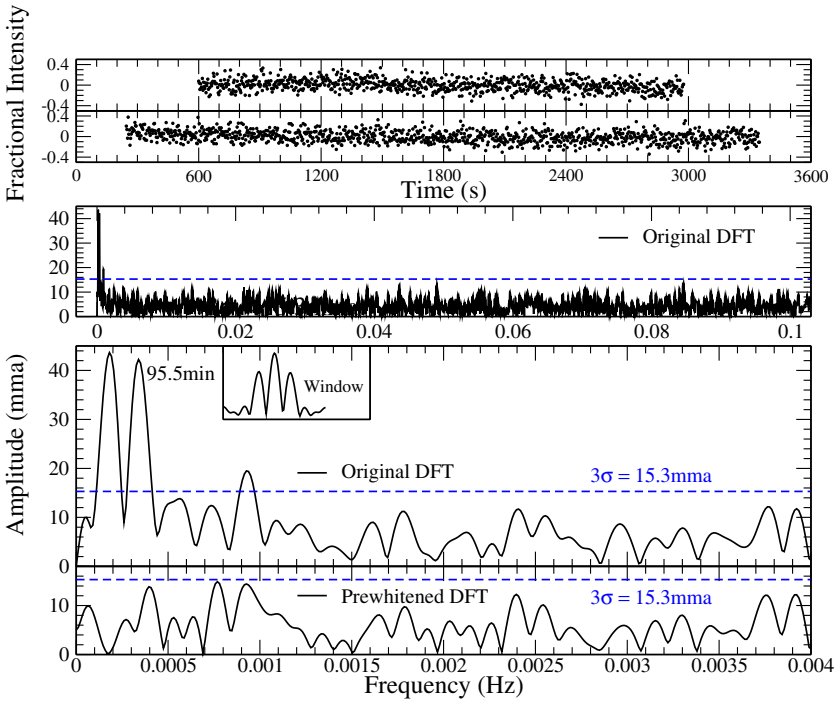

Figure 9. Ultraviolet observations of EQ Lyn acquired on 2011 March 13 reveal a period at 95.5 minutes, which may be related to the *HST* orbital period. The *HST* data show 90% of flux from the white dwarf without any evidence of pulsations.

package HSTCOS (version 3.14). We initially used the splittag routine to divide the data into 3 s bins, and then utilized the x1dcorr routine to extract the individual spectra for an optimal width of 41 pixels. Our analysis of COS time-series spectra acquired with the G140L grating revealed that an extraction width of 41 pixels reduces the noise slightly compared to the default width of 57 pixels. Next we utilized a combination of IRAF routines and our own C programs to convert these extracted spectra to text form and sum over the wavelength ranges of 1120–1208.4 Å, 1223.2–1295.6 Å, and 1312.2–1820 Å; these wavelength bins were chosen to exclude geocoronal emission features. The resultant light curve with an effective time resolution of 3 s is relatively flat (see Figure 9). The ultraviolet DFT reveals a single periodicity at 95.5 minutes, which may be related to the *HST* orbital period (Table 4). Prewhitening with the 95.5 minute period eliminates all significant power above the 3σ line (bottom panel, Figure 9).

Summing the individual spectra over time leads to a high S/N ultraviolet spectrum of EQ Lyn shown in Figure 10, which we model as a combination of the underlying white dwarf, the accretion disk, and a source of emission lines (e.g., Gänsicke et al. 2005). The fact that the observed flux in the core of Lyα does not drop to zero indicates a small contribution of the accretion disk or the hot spot. For the white dwarf, we use synthetic spectra computed with TLUSTY/SYNSPEC (Hubeny & Lanz 1995; Lanz & Hubeny 1995), spanning effective temperatures in the range of 8000–20,000 K and surface gravities in the range $7.5 \leqslant \log g \leqslant 8.5$. The exact physical nature of the low-level contribution of the accretion disk or the hot spot to the far-ultraviolet continuum is not well understood, and not constrained by our COS data. However, Szkody et al. (2010) demonstrated that this contribution can be modeled well with either a black body, a power law, or simply a constant flux offset, without noticeably affecting the white dwarf parameters. Here, we adopt a blackbody to model the disk/hot

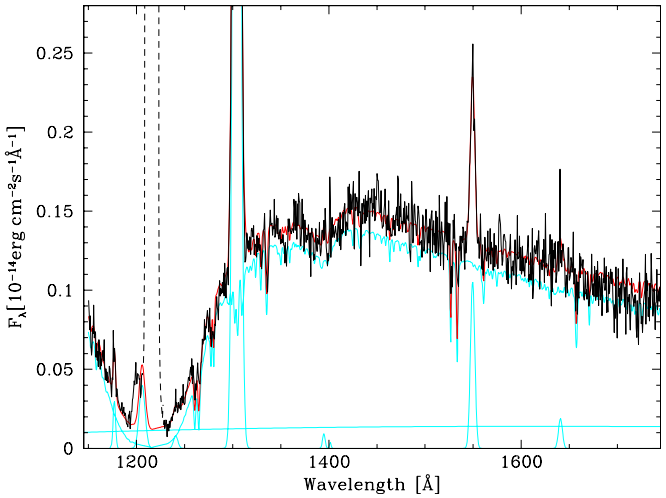

Figure 10. COS spectrum of SDSS0745 (black) along with the best-fit multi-component model (red). The individual contributions (cyan) to this model are (1) a synthetic white dwarf spectrum computed for $T_{\rm eff} = 15{,}400$ K, $\log g = 8.0$, and 0.1 times solar metal abundances; (2) a 18,000 K blackbody representing the accretion disk; and (3) Gaussian profiles for the emission lines of C III 1175 Å, Si III 1306 Å, O I 1305 Å, Si IV 1394/1403 Å, C IV 1550 Å, and He II 1640 Å. Apart from O I, all these lines are intrinsic to the system, the O I and Lyα (excluded in the fit) are of geocoronal origin.

spot continuum flux. The emission lines seen in the spectrum are fitted by Gaussian profiles, where C III 1175 Å, Si III 1306 Å, Si IV 1394/1403 Å, C IV 1550 Å, and He II 1640 Å are intrinsic to the system, and Lyα[25] and O I 1305 Å are of geocoronal origin. For a fixed value of $\log g$, the statistical uncertainty in $T_{\rm eff}$ is

[25] Lyα was excluded from the fit because it could introduce unnecessary systematic uncertainties due to its extreme strength.

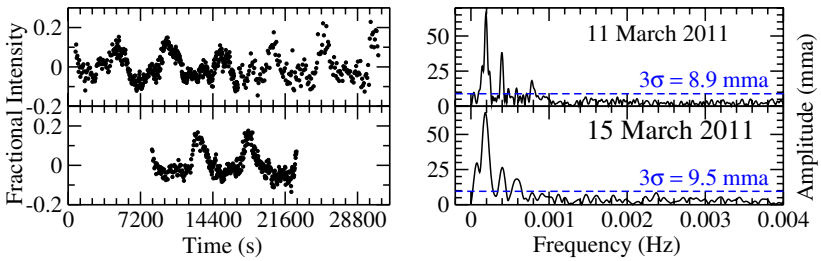

Figure 11. Optical data nearly simultaneous with the *HST* observations reveal superhumps at a period near 86 minutes and no evidence of pulsations.
(A color version and supplemental data for this figure are available in the online journal.)

of the order of 100–200 K. We are forced to assume a value of $\log g$ because we cannot constrain the stellar mass from the current data alone. For an adopted $\log g = 8$ ($M_{\rm wd} \simeq 0.6\,M_{\odot}$), we find a best-fit temperature of 15,400 K. The best-fit effective temperature and surface gravity are correlated, and adopting $\log g$ values higher (lower) by 0.5 dex results in an increase (decrease) in $T_{\rm eff}$ by $\simeq$1000 K. Hence, we adopt $\pm$1000 K as a conservative error in $T_{\rm eff}$.

The accretion disk/hot spot contribution is fit with a blackbody of 18,000 K, and contributes $\sim$10% of the far-ultraviolet continuum flux, and in turn implies that the white dwarf is the dominant ($\sim$90%) source of the ultraviolet flux. This excludes the possibility that the white dwarf was being shrouded or dominated by the accretion disk to justify the lack of pulsations, especially in the *HST* light curve.

6.2. Optical Photometry

We acquired optical time-series photometry on EQ Lyn on March 11 and 15 (Table 2) using Agile (Mukadam et al. 2011a) on the 3.5 m telescope at Apache Point Observatory (APO), and Spectral on the 2.0 m Faulkes Telescope North (FTN) of the Las Cumbres Observatory Global Telescope. The optical observations bracket the acquisition of the ultraviolet time-series spectra. The reduced data are shown in Figure 11, which reveal superhump periods near 86 minutes related to the precessing accretion disk (Table 4). Since the *HST* light curve did not reveal superhumps when optical data reveals their presence in the system, we conclude that they must originate in the outer part of the accretion disk.

7. PRELIMINARY SUGGESTION OF THE He II INSTABILITY STRIP

The pulsation characteristics of the hot ZZ Ceti stars closer to the blue edge of the instability strip are different from their compatriots near the red edge. The hot ZZ Ceti stars show relatively few pulsation modes, shorter periods around 100–350 s with low amplitudes ($\sim$0.1%–3%), and only a small degree of amplitude modulation (Clemens 1993; Kanaan et al. 2002; Mukadam et al. 2006, 2007b). Cool ZZ Ceti stars typically show relatively longer pulsation periods around 650–1000 s, larger amplitudes (up to 30%), nonlinear pulse shapes, and greater amplitude modulation (e.g., Kleinman et al. 1998). The light curves of the accreting white dwarf EQ Lyn mimic those of the non-interacting cool ZZ Ceti stars in every way. This implies that EQ Lyn lies at the red edge of the instability strip for accreting white dwarfs, if its pulsational variability is caused by nonradial g-modes.

Although the 2011 March *HST* temperature of 15,400 K was determined when EQ Lyn was not pulsating, we argue that this determination constitutes the quiescent temperature. The observed magnitude in 2011 March is consistent within the uncertainties with the quiescent magnitude observed when the star displays pulsational variability. Since the characteristic light curves of EQ Lyn imply that it is a red edge pulsator, our temperature determination then suggests that it belongs to the hotter He II instability strip. This is the first preliminary suggestion of even the existence of the He II instability strip, supporting the theoretical work done by Arras et al. (2006).

8. APPEARANCE AND DISAPPEARANCE OF PULSATIONAL VARIABILITY

We continued to monitor EQ Lyn in the Spring of 2012 (Table 2), only to find additional light curves dominated by superhumps with no evidence of pulsations (see Figure 12). Table 5 indicates the superhump periods found in our 2012 March and April observations.

Then, in 2012 December and 2013 January, pulsational variability reappeared at the periods of 1119 s and 1139 s (Figure 13). These periods, listed in Table 5, are slightly shorter than the previously observed range of 1166–1290 s, but close enough to be explicable by the excitation of adjacent radial order modes rather than those originally observed. The pulsational characteristics are essentially the same as prior to the outburst. We are unable to discern any change in the quiescent magnitude of the system within the uncertainty of 0.25 mag (caused by flickering) between the previous observations acquired during 2011 January–2012 April and the recent data acquired in 2012 December–2013 January.

Our most recent light curves obtained from 2013 March–May (Figure 13) show an absence of pulsational variability yet again. These data in conjunction with regular monitoring by the CRTS ascertain that EQ Lyn did not undergo an outburst between 2013 January and March (Figure 5). The light curve obtained on 2013 March 12 is unusual as it apparently reflects a harmonic of the orbital period as well as pulsational variability. Neither clouds nor detector failure caused the gap in this light curve, which was actually introduced by a malfunctioning instrument rotator that rotated EQ Lyn out of the field of view. Subsequent light curves from March 19 as well as April and May reflect high-amplitude superhumps at similar periods as previous observations.

9. DISCUSSION

The first step in attempting to analyze an enigmatic and elusive problem is to list all available clues.

1. The observations acquired from 2012 December to 2013 May explicitly show that pulsational variability disappears from EQ Lyn without an outburst (heating the system beyond the instability strip). The lack of a significant systematic change in magnitude between the two states

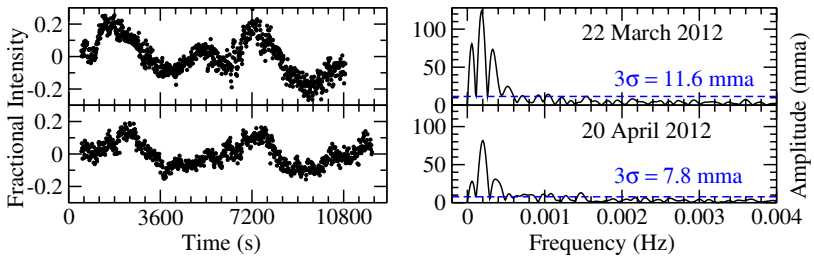

Figure 12. Optical data obtained on EQ Lyn in 2012 March–April also reveal superhumps with a period near 86 minutes and no evidence of pulsations.
(A color version and supplemental data for this figure are available in the online journal.)

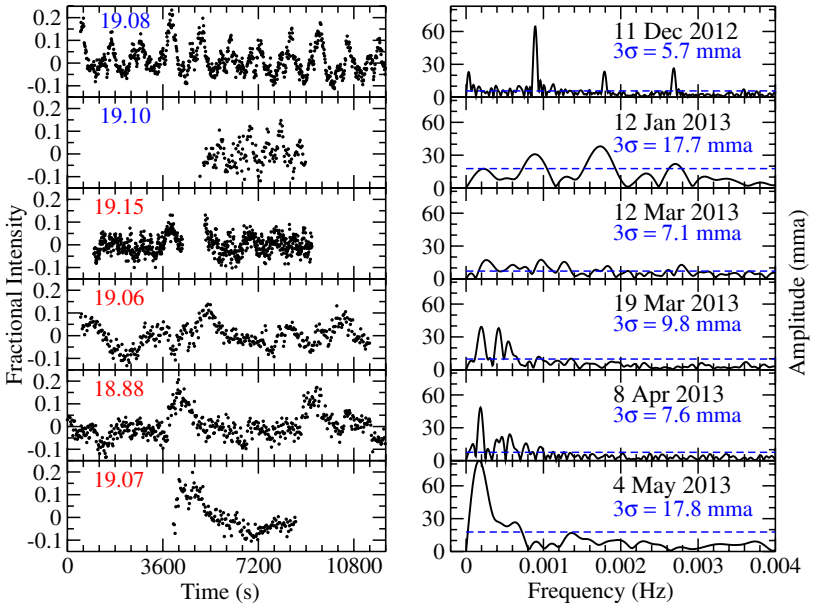

Figure 13. Recent optical data obtained on EQ Lyn from 2012 December to 2013 May reveal the initial appearance of pulsations at nearly the same period(s) as previously identified nonradial modes, as well as their subsequent disappearance in favor of superhumps.
(A color version and supplemental data for this figure are available in the online journal.)

constrains our choice of possible explanations for the observed appearance and disappearance of pulsational variability.

2. Each time the so-called high-amplitude pulsations disappear, prominent superhumps make their appearance in the light curve. This was true for the post-outburst period after 2006 October, the duration from 2011 January to 2012 April, as well as the recent period since 2013 March 19.
3. The short light curve acquired on 2013 March 12 is the very first time that we may be observing low-amplitude pulsational variability with a harmonic of the orbital period.
4. Our *HST* observations from 2011 March 13, acquired when EQ Lyn was not pulsating, reveal that 90% of the ultraviolet light from the system originated from the white dwarf.

When 90% of the observed ultraviolet flux originates from the white dwarf, and no pulsations are observed, then the white dwarf actually stopped pulsating, the pulsation amplitude became negligible due to an unfavorable inclination angle, or we are not dealing with white dwarf pulsations at all. We discuss the merits and drawbacks of each of these speculative possibilities individually.

9.1. Elevated Accretion Rate Can Heat the White Dwarf beyond the Instability Strip

An outburst heating the white dwarf out of the instability strip has already been ruled out by the CRTS monitoring during the recent season of observations between 2012 December and 2013 May (Figure 5). Our mean magnitude measurements for this duration vary by 0.25 mag (see Figure 13), and this uncertainty is consistent with the observed flickering of cataclysmic variables. Assuming that the white dwarf contributes about 60% of the optical flux, heating the white dwarf even by 2000 K would only change the observed (white light) magnitude of the cataclysmic variable by about 0.23, the limit of our observational uncertainties. Note that we do not discuss the possibility of cooling the pulsating star out of the instability strip, as the reduced accretion rate that would allow the star to cool could not explain the appearance of superhumps.

The pulsation characteristics of EQ Lyn suggest that it lies near the red edge of the instability strip. Heating a red edge pulsating white dwarf toward the middle of the instability strip is expected to cause the excitation of relatively shorter periods. Should the white dwarf be heated by the entire temperature width of the instability strip, then we would expect the pulsations to cease. There is presently no empirical information about the width of the He II instability strip for accreting white dwarfs. The well-established ZZ Ceti instability strip has a width of nearly 1500 K (Gianninas et al. 2006; Castanheira et al. 2010), while the He atmosphere DB instability strip has an implied width of nearly 6000 K (see Figure 2 of Nitta et al. 2009). If the He II instability strip has a width of $\leqslant$2000 K, only then do our magnitude measurements permit the white dwarf to be heated out of the instability strip.

The potential energy released per gram of accreted matter during infall (GM/R) is much larger than the energy released due to compressional heating. This implies that the white dwarf surface temperature can rise by 2000 K above quiescence even at the low accretion rates of $\sim 10^{-11}\ M_{\odot}\ \mathrm{yr}^{-1}$. Once the accretion rate reduces to its quiescent value, the subsequent cooling timescale is set by the total accreted mass. Matter accreted over a month would still allow cooling on thermal timescales, i.e., 10–20 minutes (Piro et al. 2005). An elevated accretion rate can cause the white dwarf to heat beyond the instability strip if its width is $\leqslant$2000 K, while perhaps also causing superhumps in the accretion disk. In such a scenario, the white dwarf would commence pulsations within minutes of the accretion rate reducing back to its normal value.

9.2. Reduced Accretion Rate Lowers the He Abundance of the Driving Region

It is the thermal timescale at the base of the convection zone that dictates the driving frequency for the excitation of pulsations (Brickhill 1992b; Goldreich & Wu 1999; Wu 2001; Montgomery 2005). Section 7 describes how the exhibition of long periods at the high temperature of 15,400 K imply that EQ Lyn may possibly belong to the red edge of the He II instability strip propounded by Arras et al. (2006). Due to the ongoing accretion, we can envisage a He-rich convection zone of uniform composition with heavier elements like He settling out at its base. Tables 5 and 6 from Paquette et al. (1986) suggest that He settles at the bottom of the convection zone on the timescales of 0.6–1.5 days in a hydrogen-rich environment for a white dwarf at 15,000 K with stellar mass in the range of 0.6–1.0 $M_{\odot}$.

Should the accretion rate reduce significantly from $10^{-11}\ M_{\odot}\ \mathrm{yr}^{-1}$ to $10^{-13}\ M_{\odot}\ \mathrm{yr}^{-1}$ for example, He will start to settle out of the convection zone on the timescales of a day, reducing its He abundance. Unlike the pure He atmosphere white dwarf DB instability strip, the boundaries of the He II instability strip also depend on He abundance, besides temperature and stellar mass (Arras et al. 2006). It is conceivable that a reduced rate of accretion could shutdown the pulsations by lowering the He abundance of the convection zone. Even at this juncture, the white dwarf photosphere could still have a thin He-rich layer, easily replenished even at the reduced rate of $\sim 10^{-13}\ M_{\odot}\ \mathrm{yr}^{-1}$. This hypothesis needs to be modeled appropriately to test whether a reduction in the accretion rate that only changes the observed magnitude by 0.25 or less is capable of disrupting white dwarf pulsations associated with the He II instability strip.

9.3. Changes in Geometry

We are unable to resolve the disk of the star from Earth. Hence, the observed amplitude of each pulsation mode is lower than the intrinsic amplitude due to a disk-averaging effect. The inclination angle of the pulsation axis dictates the distribution of the bright and dark zones in our view for a given mode, and essentially decides the observed pulsation amplitude. A highly unfavorable inclination angle can even reduce the observable amplitude to a small value beyond our detection limit, suggesting the possibility of a geometric explanation for the disappearance of pulsations.

We consider the possibility that the entire system may be precessing, causing a slow change in our viewing angle of the white dwarf and accretion disk. High-amplitude pulsations are visible when we get the best view of the pulsation pole of the white dwarf, which need not coincide with the rotational poles. It is conceivable that tidal forces impact pulsations by inclining the pulsation axis toward the companion star (Kurtz 1992; Reed & Whole Earth Telescope Xcov 21 and 23 Collaborations 2006). As the viewing angle changes, we would observe the pulsations equator-on with a minimal or negligible pulsation amplitude in the light curves. This geometric explanation works well in explaining why the observed periods always stay in the same range. If we also obtain the best view of the accretion disk when observing the pulsations equator-on, we could explain why superhumps are observed when pulsations are not.

Under this scenario, the pulsations and superhumps are always present, and their amplitudes are dictated by the varying view of the system. The longest stretches of continuous observations of EQ Lyn were obtained over a period of 11–12 days in 2006 January, when EQ Lyn was pulsating (Mukadam et al. 2011b), and 2011 January–February, when only the superhump periods were visible. For the geometric hypothesis to apply to the observations, we require that the precession period of the system be at least longer than 20–25 days. The unfortunate scarcity of our observations prevents us from placing additional constraints on the period of precession.

Leins et al. (1992) suggest that free precession could be excited in white dwarfs accreting matter from a companion. The precession period of the cataclysmic variable FS Aurigae was recently measured to be near 147 minutes (Neustroev et al. 2012; Chavez et al. 2012). A precession period at least as long as 20–25 days is well beyond the range suggested by Leins et al. (1992) for accreting white dwarfs, which indicates a period of a few hours at most. However, it may be possible to have free precession of the entire system at such long timescales. Regular monitoring of EQ Lyn with observations acquired every month would certainly help in testing the feasibility of this scenario.

9.4. Alternative Models of Pulsation

Last, but not least, we do recognize that we may be confusing accretion disk pulsations with white dwarf pulsations. The range, amplitude, and coherence of the observed periods found in accreting white dwarfs near the orbital period minimum are consistent with nonradial g-mode white dwarf pulsations, but this is not sufficient to conclude that these accreting white dwarfs are pulsating nonradially. There are alternative models of different kinds of disk and stellar pulsations that should be explored for each frequency shown by each accreting white dwarf before leaping to the model assumption of nonradial g-mode white dwarf pulsations for all observed frequencies in a suitable range.

9.4.1. Disk Pulsations

Szkody et al. (2010) report a lack of pulsations in ultraviolet light curves of REJ 1255+266, while nearly simultaneous optical observations reveal pulsational variability in these systems. While it is possible that these white dwarfs are exhibiting high ℓ g-mode pulsations,[26] it is also possible that the observed variability may be caused by axially symmetric radial p-mode

[26] Nonradial g-mode pulsations observed in white dwarfs divide the stellar surface into zones of higher and lower effective temperature, depending on the degree of spherical harmonic ℓ, thus yielding lower optical amplitudes due to a geometric cancellation effect. Increased limb darkening at ultraviolet wavelengths ensures that modes with $\ell \leqslant 3$ are canceled less effectively, leading to higher amplitudes (Robinson et al. 1995). However $\ell = 4$ modes do not show a significant change in amplitude as a function of wavelength.

pulsations trapped in the outer part of the accretion disk (e.g., Yamasaki et al. 1995), which generate periods in the range of 70–600 s.

Ortega-Rodríguez & Wagoner (2007) describe nonradial *g*-mode pulsations restricted to the inner part of the accretion disk, which would also be visible in ultraviolet light curves. However, these diskoseismic modes have periods of tens of seconds, too short to explain the observed variability in most of the accreting white dwarf pulsators. Collins et al. (2000) demonstrate that beat periods of fast torsional modes excited in the boundary layer span periods in the range of 20 s to a few hundred seconds, with underlying fundamental oscillations at ultrashort periods of order 1 s; such beat periods would also be visible in ultraviolet light curves. None of these above models of disk pulsations can presently reproduce the ∼1200 s long periods observed in EQ Lyn, however they do need to be re-examined and revised to include optically thin disks found at the low accretion rates of $\sim 10^{-11}\ M_{\odot}\ \mathrm{yr}^{-1}$ near the orbital period minimum.

9.4.2. Nonradial r-mode Pulsations

Alternatively, Saio (1982) and Papaloizou & Pringle (1978) explored *r*-mode pulsations in white dwarf stars. These pulsations are excited by the same mechanism as *g*-mode pulsations, and produce periods in the same range as the ZZ Ceti pulsation periods (Saio 1982), with the primary difference being that *g*-mode pulsations cause local temperature fluctuations, while *r*-mode pulsations would result in both temperature and velocity variations. Kepler (1984) conclude that the measurable velocity effect on the line profiles for an *r*-mode pulsation is the key in differentiating it from a *g*-mode pulsation.

Although *r*-modes have never been empirically demonstrated to exist in a white dwarf star, their observational characteristics are likely to be very similar to *g*-modes. The *r*-mode pulsation periods have to be longer than the stellar rotation period, and hence they are not interesting in the context of non-interacting white dwarf stars which rotate slowly. Rapidly rotating accreting white dwarf stars form the right environment to excite these pulsations along with nonradial *g*-modes. Without confining themselves to slow rotation, Papaloizou & Pringle (1978) calculated the eigenfrequencies of *r*-mode pulsations to be $\sigma \approx -m\Omega$, an integral multiple of the rate of rotation Ω. Modes with different radial quantum numbers would possess slightly different eigenfrequencies, similar to *g*-modes. The arguments described in Sections 9.1, 9.2, and 9.3 should also be valid for *r*-mode pulsations.

10. CONCLUSIONS

The only definitive conclusion emanating from this paper is that a substantial change in temperature associated with an outburst does not cause the disappearance of pulsational variability in EQ Lyn. What we have been able to rule out is perhaps more significant than the following speculations regarding the enigmatic observations of EQ Lyn.

1. An elevated accretion rate could sustain the white dwarf beyond the instability strip provided its width is $\leqslant$2000 K, perhaps also causing the observed superhumps during the absence of pulsational variability. Nonradial *g*-mode or *r*-mode white dwarf pulsations would be expected to resume within minutes of the accretion rate returning to its quiescent value.
2. Nonradial *g*-mode or *r*-mode white dwarf pulsations associated with the He II instability strip could get disrupted by a significant reduction in the accretion rate that effectively lowers the He abundance of the convection zone, caused by gravitational settling of He at its base on the timescale of a day. Pulsations would return as the accretion rate resumed its quiescent value. We are unable to explain the appearance of superhumps with the disappearance of pulsations in this case.
3. A geometric scenario may also be feasible, where nonradial *g*-mode or *r*-mode white dwarf pulsations appear and disappear as our changing view of the system alters the inclination angle of the pulsation axis from a favorable to an unfavorable value. Superhumps may also be appearing and disappearing due to our changing view of the disk.
4. We could be confusing two different states of the accretion disk with the appearance and disappearance of white dwarf pulsations. Most of the alternative theoretical models of disk pulsations we have presented in this paper were trying to explain quasi-periodic oscillations observed in dwarf novae, and need to be re-examined in light of the observed pulsational variability in accreting white dwarfs near the orbital period minimum with optically thin disks and low accretion rates.

We can only hope that papers such as ours lead to additional theoretical developments that can fit these observations better and either rule out or confirm the hypotheses presented here.

We thank Dr. S. O. Kepler and Dr. E. L. Robinson for intriguing and helpful conversations during the writing of this paper. A.S.M. and P.S. acknowledge the NSF for the grant AST-1008734 which provided funding for this project. Support for the program HST-GO-12231.01-A was provided by NASA through a grant from the Space Telescope Science Institute, which is operated by the Association of Universities for Research in Astronomy, Inc., under NASA contract NAS 5-26555. J.J.H., M.H.M., and D.E.W. acknowledge support from the NSF under grant AST-0909107 and the Norman Hackerman Advanced Research Program under grant 003658-0252-2009, and M.H.M. additionally acknowledges the support of NASA under grant NNX12AC96G and the Delaware Asteroseismic Research Center. This research is based on data from the CRTS survey, which is supported by the NSF under the grant AST-0909182. The CSS survey is funded by NASA under the grant NNG05GF22G issued through the Science Mission Directorate Near-Earth Objects Observations Program. We thank the Las Cumbres Observatory for time on the 2 m FTN.

REFERENCES

Araujo-Betancor, S., Gänsicke, B. T., Hagen, H.-J., et al. 2005, A&A, 430, 629
Arras, P., Townsley, D. M., & Bildsten, L. 2006, ApJL, 643, L119
Bailey, J. 1979, MNRAS, 189, 41P
Bergeron, P., Fontaine, G., Billères, M., Boudreault, S., & Green, E. M. 2004, ApJ, 600, 404
Brassard, P., Fontaine, G., & Wesemael, F. 1995, ApJS, 96, 545
Breedt, E., Gänsicke, B. T., Marsh, T. R., et al. 2012, MNRAS, 425, 2548
Brickhill, A. J. 1992a, MNRAS, 259, 529
Brickhill, A. J. 1992b, MNRAS, 259, 519
Castanheira, B. G., Kepler, S. O., Kleinman, S. J., Nitta, A., & Fraga, L. 2010, MNRAS, 405, 2561
Chavez, C. E., Tovmassian, G., Aguilar, L. A., Zharikov, S., & Henden, A. A. 2012, A&A, 538, A122
Clemens, J. C. 1993, BaltA, 2, 407
Collins, T. J. B., Helfer, H. L., & Van Horn, H. M. 2000, ApJ, 534, 944
Downes, R. A. 1990, AJ, 99, 339

Drake, A. J., Djorgovski, S. G., Mahabal, A., et al. 2009, ApJ, 696, 870
Fontaine, G., & Brassard, P. 2008, PASP, 120, 1043
Friend, M. T., Smith, R. C., Martin, J. S., & Jones, D. H. P. 1988, MNRAS, 233, 451
Gänsicke, B. T., Dillon, M., Southworth, J., et al. 2009, MNRAS, 397, 2170
Gänsicke, B. T., Rodríguez-Gil, P., Marsh, T. R., et al. 2006, MNRAS, 365, 969
Gänsicke, B. T., Sion, E. M., Beuermann, K., et al. 1999, A&A, 347, 178
Gänsicke, B. T., Szkody, P., Howell, S. B., & Sion, E. M. 2005, ApJ, 629, 451
Gianninas, A., Bergeron, P., & Fontaine, G. 2006, AJ, 132, 831
Goldreich, P., & Wu, Y. 1999, ApJ, 511, 904
Howell, S. B., Szkody, P., & Cannizzo, J. K. 1995, ApJ, 439, 337
Hubeny, I., & Lanz, T. 1995, ApJ, 439, 875
Kanaan, A., Kepler, S. O., & Winget, D. E. 2002, A&A, 389, 896
Kato, T., Imada, A., Uemura, M., et al. 2009, PASJ, 61, 395
Kato, T., Maehara, H., & Monard, B. 2008, PASJ, 60, L23
Kato, T., Sekine, Y., & Hirata, R. 2001, PASJ, 53, 1191
Kepler, S. O. 1984, ApJ, 286, 314
Kleinman, S. J., Nather, R. E., Winget, D. E., et al. 1998, ApJ, 495, 424
Koester, D., & Holberg, J. B. 2001, in ASP Conf. Ser. 226, 12th European Workshop on White Dwarfs, ed. J. L. Provencal, H. L. Shipman, J. MacDonald, & S. Goodchild (San Francisco, CA: ASP), 299
Kolb, U., & Baraffe, I. 1999, MNRAS, 309, 1034
Kurtz, D. W. 1992, MNRAS, 259, 701
Lanz, T., & Hubeny, I. 1995, ApJ, 439, 905
Leins, M., Soffel, M. H., Lay, W., & Ruder, H. 1992, A&A, 261, 658
Marsh, T. R. 1989, PASP, 101, 1032
Montgomery, M. H. 2005, ApJ, 633, 1142
Montgomery, M. H., Provencal, J. L., Kanaan, A., et al. 2010, ApJ, 716, 84
Mukadam, A. S., Gänsicke, B. T., Szkody, P., et al. 2007a, ApJ, 667, 433
Mukadam, A. S., Montgomery, M. H., Kim, A., et al. 2007b, in ASP Conf. Ser. 372, 15th European Workshop on White Dwarfs, ed. R. Napiwotzki & M. R. Burleigh (San Francisco, CA: ASP), 587
Mukadam, A. S., Montgomery, M. H., Winget, D. E., Kepler, S. O., & Clemens, J. C. 2006, ApJ, 640, 956
Mukadam, A. S., Owen, R., Mannery, E., et al. 2011a, PASP, 123, 1423
Mukadam, A. S., Townsley, D. M., Szkody, P., et al. 2011b, ApJL, 728, L33
Mukadam, A. S., Winget, D. E., von Hippel, T., et al. 2004, ApJ, 612, 1052
Nelemans, G. 2005, in ASP Conf. Ser. 330, The Astrophysics of Cataclysmic Variables and Related Objects, ed. J.-M. Hameury & J.-P. Lasota (San Francisco, CA: ASP), 27
Neustroev, V., Tovmassian, G., Zharikov, S., et al. 2012, MmSAI, 83, 724
Nitta, A., Kleinman, S. J., Krzesinski, J., et al. 2009, ApJ, 690, 560
O'Donoghue, D., Kanaan, A., Kleinman, S. J., Krzesinski, J., & Pritchet, C. 2000, BaltA, 9, 375
Ortega-Rodríguez, M., & Wagoner, R. V. 2007, ApJ, 668, 1158
Papaloizou, J., & Pringle, J. E. 1978, MNRAS, 182, 423
Paquette, C., Pelletier, C., Fontaine, G., & Michaud, G. 1986, ApJS, 61, 197
Patterson, J., Kemp, J., Harvey, D. A., et al. 2005, PASP, 117, 1204
Patterson, J., Thorstensen, J. R., & Knigge, C. 2008, PASP, 120, 510
Pavlenko, E. 2009, JPhCS, 172, 012071
Piro, A. L., Arras, P., & Bildsten, L. 2005, ApJ, 628, 401
Provencal, J. L., Montgomery, M. H., Kanaan, A., et al. 2012, ApJ, 751, 91
Reed, M. D., & Whole Earth Telescope Xcov 21 and 23 Collaborations. 2006, MmSAI, 77, 417
Robinson, E. L., Mailloux, T. M., Zhang, E., et al. 1995, ApJ, 438, 908
Roelofs, G. H. A., Rau, A., Marsh, T. R., et al. 2010, ApJL, 711, L138
Saio, H. 1982, ApJ, 256, 717
Schneider, D. P., & Young, P. 1980, ApJ, 238, 946
Szkody, P., Henden, A., Agüeros, M., et al. 2006, AJ, 131, 973
Szkody, P., Mukadam, A., Gänsicke, B. T., et al. 2007, ApJ, 658, 1188
Szkody, P., Mukadam, A., Gänsicke, B. T., et al. 2010, ApJ, 710, 64
Szkody, P., Mukadam, A. S., Gänsicke, B. T., et al. 2012, ApJ, 753, 158
Tody, D. 1993, in ASP Conf. Ser. 52, Astronomical Data Analysis Software and Systems II, ed. R. J. Hanisch, R. J. V. Brissenden, & J. Barnes (San Francisco, CA: ASP), 173
Townsley, D. M., Arras, P., & Bildsten, L. 2004, ApJL, 608, L105
Uemura, M., Kato, T., Nogami, D., & Ohsugi, T. 2010, PASJ, 62, 613
van Zyl, L., Warner, B., O'Donoghue, D., et al. 2004, MNRAS, 350, 307
Vanlandingham, K. M., Schwarz, G. J., & Howell, S. B. 2005, PASP, 117, 928
Warner, B. 1995, Cataclysmic Variable Stars (Cambridge Astrophysics Series, vol. 28; Cambridge: Cambridge Univ. Press)
Warner, B., & van Zyl, L. 1998, in IAU Symp. 185, New Eyes to See Inside the Sun and Stars, ed. F.-L. Deubner, J. Christensen-Dalsgaard, & D. Kurtz (Cambridge: Cambridge Univ. Press), 321
Winget, D. E., & Kepler, S. O. 2008, ARA&A, 46, 157
Winget, D. E., Nather, R. E., Clemens, J. C., et al. 1994, ApJ, 430, 839
Wu, Y. 2001, MNRAS, 323, 248
Yamasaki, T., Kato, S., & Mineshige, S. 1995, PASJ, 47, 59